

1 **Evolution of salt structures during extension and inversion of the**
2 **Offshore Parentis Basin (Eastern Bay of Biscay)**

3
4 Ferrer, O. ^{(1)*}; Jackson, M. P. A. ⁽²⁾; Roca, E. ⁽¹⁾ and Rubinat, M. ⁽¹⁾

5
6 ⁽¹⁾ GEOMODELS Research Institute, Departament de Geodinàmica i Geofísica, Facultat de Geologia,
7 Universitat de Barcelona, C/ Martí i Franquès s/n, 08028 Barcelona, Spain

8 ⁽²⁾ Bureau of Economic Geology, Jackson School of Geosciences, University of Texas at Austin,
9 University Station, Box X, Austin, Texas 78713-8324, U.S.A

10
11 * Corresponding author. Fax: +34934021340, E-mail: joferrer@ub.edu

12
13 Abbreviated title: **Salt Structures Parentis Basin**

14 **8888 words of text, 71 references and 12 figures**

15
16 **Keywords:** salt diapir, salt tectonics, inversion, Parentis Basin, Bay of Biscay.

17
18 **Abstract**

19
20 The Late Jurassic-Cretaceous Parentis Basin (Eastern Bay of Biscay) illustrates a
21 complex geological interplay between crustal tectonics and salt tectonics. Salt structures
22 are mainly near the edges of the basin, where Jurassic-Lower Cretaceous overburden is
23 thinner than in the basin centre and allowed salt anticlines and diapirs to form.

24 Salt diapirs and walls began to rise reactively during the Late Jurassic as the
25 North Atlantic Ocean and the Bay of Biscay opened. Some salt-cored drape folds
26 formed above basement faults from the Upper Jurassic to Albian. During Albian-Late

27 Cretaceous times, passive salt diapirs rose in chains of massive salt walls. Many salt
28 diapirs stopped growing in the mid-Cretaceous when their source layer depleted. During
29 the Pyrenean orogeny (Late Cretaceous-Cenozoic) the basin was mildly shortened. Salt
30 structures absorbed almost all the shortening and were rejuvenated to form squeezed
31 diapirs, salt glaciers, and probably subvertical welds, some of which were later
32 reactivated as reverse faults. No new diapirs formed during the Pyrenean compression,
33 and salt tectonics ended with the close of the Pyrenean orogeny in the Middle Miocene.

34 Using reprocessed industrial seismic surveys, we document how salt tectonics
35 affected the structural evolution of this offshore basin largely unknown to the
36 international audience.

37

38 **Introduction**

39 During the last decade or two, the important role of salt in facilitating shortening
40 in sedimentary basins has been highlighted with examples around the world (for
41 references, see reviews by [Jackson, 1995](#), [Letouzey et al., 1995](#), [Rowan et al., 2004](#) and
42 [Hudec & Jackson, 2007](#)). Many studies have focused on the salt-related effects of strong
43 shortening, but much less work has addressed the subtler effects of mild shortening of
44 salt structures. A subset of studies has focused on three types of salt tectonics: inversion
45 controlled by basement faults (e.g., [Stefanescu et al., 2000](#); [Stewart, 2007](#)); thin-skinned
46 salt structures over a detachment (e.g., [Brun & Fort, 2004](#); [Rowan et al., 2004](#); [Sherkati
47 et al., 2006](#)); and salt-cored drape folds associated with extensional basement faults
48 (e.g., [Withjack & Callaway, 2000](#)). The Parentis Basin has all three types of salt
49 tectonics and is an excellent example of salt structures mildly affected by regional
50 compression.

51 The Parentis Basin is in the northern foreland of the Pyrenean chain. In this
52 basin salt structures were grown during Jurassic-Cretaceous rifting as the Bay of Biscay
53 and the North Atlantic Ocean began to open and were subsequently inverted when the
54 Iberian and Eurasian plates collided and Pyrenean shortening propagated northwards
55 into the Parentis Basin in the late Cretaceous and Paleogene.

56 This basin is a western continuation of the onshore Aquitaine region
57 (southwestern France) and widens westward into the Bay of Biscay (Figs. 1A & 1B).
58 The eastern Bay of Biscay has two bathymetric domains separated by a bathymetric step
59 (e.g. Sibuet *et al.* 2004a): a shallow part represented by the Landes shelf having a
60 maximum depth of 200 m and the Landes Plateau between 200 and 1500 m deep (Fig.
61 2).

62 The Parentis Basin has been explored for petroleum for more than 50 years.
63 Onshore exploration started in 1953 and in 1954 discovered the Parentis field
64 (210.000.000 BBL of oil) (Biteau *et al.*, 2006). Offshore exploration drilling started in
65 1966 (Bourrouilh *et al.*, 1995; Le Vot *et al.*, 1996). The Parentis Basin has become a
66 major oil-producing province in France with accumulations in carbonate reservoirs of
67 Upper Jurassic to Lower Cretaceous sandstones. Most oil fields discovered are onshore
68 (Parentis, Cazaux, Les Arbousiers, Les Pins, Lugos, Mothes, Lucats, Courbey, Tamaris
69 and Les Mimosas), and no significant oil or gas has been reported offshore (Masclé *et*
70 *al.*, 1994; Biteau *et al.*, 2006). After lack of success, offshore exploration decreased and
71 some 3D-seismic surveys have been released since the 1990s in the shallow offshore. In
72 contrast to the onshore and in the shallow offshore, the deep offshore (>200 m depth)
73 has been little explored. 2D-seismic surveys have been carried out, but no exploration
74 wells have been drilled in the deep offshore (Fig. 2).

75 Although salt tectonics was important in the evolution of the basin, no
76 publications have addressed this role in the entire offshore Parentis Basin. Several
77 studies have covered the structural evolution of the basin (Mathieu, 1986; Mascle *et al.*,
78 1994; Biteau *et al.*, 2006); others have focused only on some salt structures in the
79 eastern part of the basin (Curnelle & Marco, 1983; Mariaud, 1987; Mediavilla, 1987). In
80 addition, these studies concentrated in the French part of the basin, neglecting the
81 Spanish part against the North Iberian margin.

82 Using conventional recently reprocessed 2D seismic surveys and well data from
83 the Parentis Basin, we present new interpretations of the timing of the main tectonic
84 domains and the style and evolution of salt structures, focusing on extension of the
85 continental margins and the subsequent Pyrenean inversion.

86

87 **Geological and structural setting**

88 The Bay of Biscay is an E–W oriented embayment of the Atlantic Ocean
89 between the Iberian Peninsula and the western coast of France (Fig. 1A & 1B). The bay
90 opened between late Barremian and Santonian times (e.g. Montadert *et al.*, 1979; Le
91 Pichon & Barbier, 1987; García-Mondejar, 1996; Vergés & García-Senz, 2001; Sibuet
92 *et al.*, 2004b). The Bay of Biscay has two distinct domains. The western domain is an
93 abyssal plain 4–5 km deep underlain by transitional to oceanic crust (Gallastegui *et al.*,
94 2002; Thinon *et al.*, 2003; Sibuet *et al.*, 2004a, 2004b; Pedreira, 2004; Ruiz, 2007). The
95 eastern domain is a shallow shelf and an intermediate plateau overlying continental
96 crust 15–25 km thick (Pinet *et al.*, 1987; Ruiz, 2007). Both domains are bounded to the
97 north-east by the Armorican Margin (Figs. 1B & 3), which is a Mesozoic passive
98 margin having southwest-verging normal listric faults (Montadert *et al.*, 1979;
99 Deregnacourt & Boillot, 1982; Le Pichon & Barbier, 1987; Thinon *et al.*, 2003). The

100 southern boundary of the Bay of Biscay is the North Iberian Margin (Figs. 1B & 3), a
101 north-verging basement-involved thrust system of Late Cretaceous-Cenozoic age that
102 overthrust Paleozoic to Cenozoic sediments of the Bay of Biscay abyssal plain (e.g.
103 Sibuet *et al.*, 1971; Boillot, 1986; Álvarez-Marrón *et al.*, 1996; Gallastegui *et al.*, 2002;
104 Ayarza *et al.*, 2004, Pedreira, 2004) (Fig. 1C). This thrust system is the northern front of
105 the Pyrenean orogen, which separates the Iberian and the Eurasian plates (Fig. 1B &
106 1C). Adjoining this front is the North Pyrenean foreland basin which preserves the
107 Mesozoic Parentis Basin in the eastern Bay of Biscay (Figs. 1C).

108 The Parentis Basin includes four bathymetric domains: the Landes shelf, the
109 Armorican shelf, the Basque shelf and the deeper Landes Plateau enclosed by them
110 (Fig. 2). The southern Parentis Basin is bounded by the major north-dipping Ibis and
111 Landes faults, visible in the ECORS-Bay of Biscay and MARCONI-3 profiles (Figs. 3,
112 4A & 4B). In the Ibis area (Fig. 4A), the basin is only 40 km wide, but the extensional
113 faults have up to 2 s two-way time (about 3400 m) throw (Bois *et al.*, 1997). However,
114 farther west (Fig. 4B), the basin widens to 70 km, and the extensional faults have less
115 throw.

116 To the south of the main faults, the Landes High (Fig. 1B) is part of a plateau
117 uplifted and eroded with an uppermost Cretaceous–Cenozoic thick sedimentary
118 succession that unconformably overlies Hercynian basement or a thin and partially
119 eroded Triassic–Jurassic cover (Gariel *et al.*, 1997) (Fig. 1C). To the north, the basin is
120 limited by the Celt-Aquitaine Flexure, a hinge line (Fig. 3). South of this hinge the pre-
121 Triassic basement is deepest and the Mesozoic and Cenozoic fill is thickest.

122 The Parentis Basin contains Mesozoic and Cenozoic strata nearly 15 km thick
123 (Dardel & Rosset, 1971; Mathieu, 1986; Bourrouilh *et al.*, 1995; Bois & Gariel, 1994;
124 Bois *et al.*, 1997) (Fig. 5). East-striking normal faults offset the Mesozoic succession

125 (Masse, 1997), and diapirs of upper Triassic evaporites pierce the basin fill (Curnelle &
126 Marco, 1983; Mathieu, 1986; Mediavilla, 1987; Ferrer *et al.*, 2008a), including the
127 Upper Cretaceous to Cenozoic synorogenic deposits (Curnelle & Marco, 1983; Bois *et*
128 *al.*, 1997; Masse, 1997; Ferrer *et al.* 2008a) (Fig. 4A).

129 The Moho shallows northwards from about 30-35 km beneath the Basque shelf
130 to 18-22 km below the Cap Ferret Canyon along the E-W boundary between the Landes
131 Plateau and the Armorican shelf (Fig. 1C). North of this boundary, the Moho abruptly
132 deepens to 30-36 km beneath the Armorican shelf (Roberts & Montadert, 1980;
133 Tomassino & Marillier, 1997; Thinon *et al.*, 2003). The crustal thickness decreases
134 westwards from 7 km in the ECORS Bay of Biscay (Pinet *et al.*, 1987; Tomassino &
135 Marillier, 1997) (Fig. 4A) to 6-5 km in the MARCONI-3 profile (Gallart *et al.*, 2004;
136 Ruiz, 2007) (Figs. 1C & 4B).

137 The formation and evolution of the Parentis Basin was controlled by the relative
138 motion of the Iberian and Eurasian plates as the North Atlantic Ocean opened. Two
139 rifting episodes (Permian-Triassic and latest Jurassic-Lower Cretaceous) related to the
140 break-up of Pangea formed a transtensional to extensional plate boundary between
141 Iberia and Eurasia (Srivastava *et al.*, 1990). The main Mesozoic sub-basins north of the
142 Pyrenees formed, among them the Parentis Basin (Curnelle *et al.*, 1982; Bourrouilh *et*
143 *al.*, 1995; Biteau *et al.*, 2006). The main depocentre of the Parentis Basin formed from
144 the Barremian to middle Albian (Fig. 4A). From late Santonian, faster opening of the
145 South Atlantic Ocean and increased northward translation of the African plate caused
146 the Iberian and Eurasian plates to converge then collide (Ziegler, 1988; Rosenbaum *et*
147 *al.*, 2002) and partially closed the Bay of Biscay. Although Pyrenean collision inverted
148 the most important Mesozoic Pyrenean extensional basins along the Iberian-European
149 plates boundary (e.g. Basque-Cantabrian, Lacq-Mauleon or Organyà basins)

150 (Choukroune & ECORS Team, 1989; Roure *et al.*, 1989; Muñoz, 1992, Álvarez-Marrón
151 *et al.*, 1996; Bourrouilh *et al.*, 1995), the Parentis Basin was only slightly inverted
152 (Mathieu, 1986; Pinet *et al.*, 1987; Bois & ECORS Scientific Party, 1990; Verges &
153 García-Senz, 2001), probably because the Landes High blocked northward propagation
154 of Pyrenean shortening (Fig. 1C) (Ferrer *et al.*, 2008a). This buttressing may have been
155 induced by stronger or thicker crust below the Landes High.

156

157 **Dataset and methodology**

158 The seismic dataset comprised 12 reprocessed 2D conventional seismic lines
159 shot between 1974 and 1990 and two reprocessed deep seismic surveys (ECORS and
160 MARCONI), covering almost all the Eastern Bay of Biscay, except part of the northern
161 Parentis Basin, the Armorican extensional margin and the deep offshore (Fig. 2). Recent
162 reprocessing of conventional seismic data has significantly improved imaging,
163 especially of allochthonous salt. However, the top and the base of the autochthonous
164 salt are still poorly imaged in many seismic profiles and in places interpretation is
165 merely speculative.

166 Twenty three wells constrain seismic interpretation in the eastern Parentis Basin
167 (Fig. 2). Because of water depths of >1000 m, no wells have been drilled in the western
168 part of the basin, so surveys there have been correlated from wells in the east.

169

170 **Salt-related structures**

171 The offshore Parentis Basin exhibits a wide array of salt-related structures.
172 Triassic Keuper salt or its welded equivalent underlies the entire Parentis Basin within
173 the study area. The ECORS-Bay of Biscay profile illustrates the structural style of the
174 eastern Parentis Basin domain (Fig. 4A). Here the basin is asymmetrical and its deepest

175 part overlies the thinnest crust. This thinning was controlled by the Ibis Fault whose slip
176 tilted the hanging wall to the south. Salt walls or salt anticlines cluster along the edges
177 of the Parentis Basin (Fig. 3), where the overburden is thinnest. The viscous salt layer
178 accommodated an extensional drape (forced) fold above the Ibis Fault.

179 Conversely, the basin geometry is different in the west, as shown by the
180 MARCONI-3 seismic profile (Fig. 4B) 52 km farther west. Instead of merely pinching
181 out, the basin ends abruptly with a half-graben controlled by a major north-dipping fault
182 (Landes Fault). The half-graben is filled by thick Jurassic-Upper Cretaceous carbonates
183 deformed by ENE-trending salt-cored anticlines and squeezed salt walls near the master
184 fault (Ferrer *et al.*, 2008a). In contrast to those farther east, salt-cored anticlines have
185 longer wavelength (up to 10 km), amplitude and lateral continuity (between 15 and 20
186 km).

187

188 *Eastern domain*

189 In the eastern domain the deepest part of the basin is the Parentis Trough (nearly
190 12 km deep) (dash blue line in Fig. 3), a syncline trending east for more than 30 km.
191 The trough results from extension on the Ibis Fault between the Neocomian and the
192 early Albian and from deformation of the Keuper evaporites and its overburden. This
193 trough continues eastwards in the onshore Parentis Basin (Fig. 3). The thickness of
194 Lower Cretaceous sediments reaches more than 3400 m in the hanging wall of the Ibis
195 Fault, where the fault has a throw of about 2500 m.

196 Salt structures of contrasting geometry formed near the northern and southern
197 basin margins. In the north, gentle salt-cored anticlines trending WNW deform all the
198 Mesozoic sequences, which were mildly flexed across the northern basin-margin hinge
199 (Céphée-Aldeberan Ridge) (Figs. 3 & 6). Conversely in the southern margin, salt

200 structures are more complex and include ENE-trending salt anticlines (Eridan-Antares
201 Ridge), diapiric salt walls, isolated teardrop diapirs, stocks and allochthonous salt sheets
202 (Figs. 3, 6, 7 & 8). These salt structures affect Mesozoic and Cenozoic strata.

203 Along the southern margin of the Parentis Trough, the Ibis/Eridan-Antares
204 ridges comprise salt-cored anticlines along the Ibis Fault and deform only Mesozoic
205 strata. These ridges stretch 55 km and trend WNW near the French coast to ENE farther
206 west (Fig. 3). Folded strata include a thick Jurassic unit, a Lower Cretaceous unit that
207 thickens in the Parentis Trough, and an Albian-Upper Cretaceous unit that thickens
208 markedly north of the anticline (Fig. 6). These last syn-folding deposits are cut by
209 north-verging break thrusts in the northern limbs of the salt-cored anticlines. The
210 structural complexity of the Eridan-Antarés anticline increases towards the east, where
211 its north flank is highly faulted. In the southern limb of the anticline the Jurassic-
212 Cretaceous transition is marked by southward thinning and the onlapping of Lower
213 Cretaceous strata. Farther south, a strongly erosive regional unconformity marks this
214 transition.

215 South of the Ibis/Eridan-Antares ridges, the apparent narrowness and inverted
216 tear drop shape of ENE-trending salt ridges, such as Alcyon and Puffin, suggest that the
217 diapirs were squeezed or even welded (Fig. 6). The bulbs overlie what we interpret as
218 subvertical secondary salt welds, formed by pinching off of the diapir stems during
219 lateral compression.

220 Lateral cutoffs of adjoining strata suggest that these salt walls grew as passive
221 diapirs from Jurassic to early Miocene times. These diapirs are associated with minor
222 north-dipping normal faults displacing the Jurassic and Lower Cretaceous series and
223 apparently detached in the Upper Triassic evaporites. No diapirs reach the present sea
224 floor.

225 One of these salt walls extruded to form the large Pelican Salt Sheet (Figs. 3 &
226 7) in the central part of the basin. Stratal cutoffs against the base of the sheet suggest
227 ~20 km of advance of salt, probably by extruding as a glacier over the sea floor
228 (Fletcher *et al.*, 1995; Hudec & Jackson, 2006). Cutoffs show that the Pelican Salt Sheet
229 began to spread at the end of Albian time and extruded farthest in Paleocene-Eocene
230 times during the Pyrenean orogeny. Regional shortening typically squeezes and expels
231 salt from diapirs to form a vigorous salt extrusion at the surface (Jackson & Cramez,
232 1989; Letouzey & Sherkati, 2004; Hudec & Jackson, 2006; Callot *et al.*, 2007). The
233 Ibis-2 well drilled nearly 250 m of Triassic salt in this salt-sheet between Eocene strata
234 below and Senonian strata above. These Senonian rocks have been interpreted as a
235 dismembered roof fragment carried during salt extrusion (Curnelle & Marco, 1983).
236 Sporadic normal faults above the salt-sheet suggest accommodation of the overburden
237 as salt was redistributed within the buried allochthonous sheet. The thin sedimentary
238 roof of this structure was stretched by flow of underlying salt. Gentle folds in the roof of
239 the Pelican structure indicate continued flow within the salt sheet caused by differential
240 loading of the overburden or by Pyrenean shortening (Fig. 7). Well data indicate that
241 this salt-sheet stopped advancing and was buried during the Oligocene, probably
242 because its feeder stem finally pinched shut during the Pyrenean shortening.

243

244 *Western domain*

245 Unlike the eastern domain, the western domain of the Parentis Basin (Fig. 3 &
246 4B), widens and is filled by thicker (5000–8500 m) Jurassic-Lower Cretaceous
247 sequences overlain by an uppermost Cretaceous-Cenozoic package (Ferrer *et al.*,
248 2008a). The southern boundary of the basin is the major Landes Fault (Fig. 4B), which
249 lies southwest of the Ibis Fault (Ferrer *et al.*, 2008a) (Fig. 3). The footwall of the Landes

250 Fault tilts south, whereas the hanging wall is either broadly anticlinal (Fig. 4B) or near
251 horizontal (Fig. 9). The dominant structures in this domain, which trend ENE, are the
252 Izurde, Marratxo and Txipiroi anticlines defined by Jurassic-Lower Cretaceous
253 overburden and cored by Upper Triassic evaporites (Fig. 9). These folds have a greater
254 wavelength (up to 10 km), amplitude and lateral continuity (between 15 and 20 km)
255 than do the eastern basin ridges. The Txipiroi salt-anticline overlies a gentle basement
256 antiform (Fig. 4B). In contrast the Marratxo and Izurde salt anticlines formed where the
257 basement was virtually flat (Fig. 9). Despite the different basement structure, these
258 structures share the following features.

- 259 • The Jurassic-Aptian successions were extended by north-dipping normal faults
260 detached in the Upper Triassic evaporites. These faults are located mainly in the
261 northern flank of the anticlines, especially near the synclinal hinges (Fig. 9).
- 262 • In the southern flanks of these structures a strong erosional unconformity across
263 the Lower and Upper Cretaceous successions is overlain by uppermost
264 Cretaceous-Paleocene strata.
- 265 • The uppermost Cretaceous-Cenozoic units thin towards the crest of salt
266 anticlines on both sides, suggesting that the fold limbs rotated during Pyrenean
267 shortening.
- 268 • Salt anticlines are separated by autochthonous salt thinned to the point of
269 welding (Fig. 9). Some of these salt anticlines may have produced salt diapirs, as
270 in the crest of the Izurde Ridge (Fig. 9).

271 In the western domain diapirs are close to the Landes Fault (Figs. 9 & 10). Their bulbs
272 have an inverted-teardrop shape suggesting a secondary near-vertical weld formed by
273 closing of the diapir stem (Fig. 10). Although mechanically feasible, the presence of
274 welded feeders is speculative because of poor data quality. These diapirs cut most of the

275 folded Albian and Lower Cretaceous reflectors but only some uppermost Albian and
276 Upper Cretaceous reflectors. Although seismic resolution is poor, some diapiric
277 pedestals are interpreted at the base of the secondary welds.

278 Study of the Ibis and Landes faults is outside the scope of this paper and both
279 structures have poor seismic coverage (Fig. 2). Nevertheless we provisionally interpret
280 the Ibis and Landes faults as a large relay structure in which the Triassic salt and its
281 diapirs are confined to the hanging wall of the Landes Fault but extend eastwards up
282 the relay ramp into the footwall of the Ibis Fault (Fig. 3).

283

284 **Initiation and growth of salt diapirs**

285 Due to poor seismic resolution at depth, diapiric initiation is poorly documented.
286 However, in some cases cutoffs of flanking reflectors suggest that salt diapirs and walls
287 began to rise during the Late Jurassic. These diapirs could have been initiated reactively
288 by mild extension of the carbonate platform during post-rift thermal subsidence (Fig.
289 11). In the most cases, the actual normal faults that could have initiated reactive
290 diapirism are not clearly imaged, and so our interpretation is conjectural. Nonetheless, a
291 large reactive diapir is preserved in the western Parentis domain between Euskal Balea
292 and Izurde ridges (Fig. 9). Differential thicknesses of growth strata on its flanks suggest
293 that it began rising in the Jurassic. Abundant Late Jurassic-Early Cretaceous normal
294 faults between diapirs support an extensional setting (Fig. 9).

295 Some diapirs could have been triggered by differential sedimentary loading
296 because the Upper Jurassic sequence varies slightly in thickness (Figs. 6–8). More
297 severe tectonic instability is suggested by the major unconformity at the Jurassic-
298 Cretaceous transition along both edges of the eastern Parentis domain (Mathieu, 1986;
299 Mediavialla, 1987; Masse, 1997; Biteau *et al.*, 2006). Farther south, in the Alcyon or

300 Puffin zone, this erosion exposed Middle Jurassic strata (Figs. 6, 8, 12b & 12c). This
301 erosive unconformity has been linked to the growth of salt anticlines during Triassic-
302 Liassic deformation (Curnelle & Cabanis, 1989) but could also record uplift of a rift
303 shoulder as the Bay of Biscay began to open in the Cretaceous. This rifting could have
304 initiated reactive diapirism.

305 As subsidence peaked, a 5-km-thick Barremian to Albian sequence filled the
306 Parentis Trough (Brunet, 1991) (Figs. 12b, 12c & 12d). Sediment loading in the Parentis
307 Trough expelled Keuper evaporites towards the edges of the basin, where salt-cored
308 anticlines formed (Eridan-Antares-Ibis in the southern and Céphée-Castor in the
309 northern area) (Figs 11, 12c & 12d). Because Jurassic-Lower Cretaceous aggradation
310 was faster in the west, salt diapirs there tended not to reach the surface or extrude. Deep
311 diapirs grew in the footwall of extensional faults, forming broad but low diapirs.
312 Exceptions were the relatively tall diapirs, Euskal Balea and Izurde. To the south the
313 Basque-Cantabrian shelf remained high during the Lower Cretaceous (Mathieu, 1986;
314 Bois *et al.*, 1997). Some reefs grew above the salt-cored anticlines (e.g., Antares) of the
315 northern Parentis edge during the mid-upper Albian (Mathieu, 1986; Biteau *et al.*,
316 2006). The distribution of these carbonate buildups in the shelf margin was probably
317 controlled by the interaction of eustasy, salt tectonics and paleogeography, as in the
318 Mesozoic La Popa Basin (Mexico) and the modern Persian Gulf (Purser, 1973; Giles &
319 Lawton, 2002).

320 During the Albian-Late Cretaceous, salt diapirs rose in chains of massive salt
321 walls (Figs 12d & 12e). Once they pierced reactively to the surface, the salt walls would
322 have continued to grow as passive diapirs (Fig. 11). Most diapirs have thickened
323 peripheral sinks of Albian-Upper Cretaceous age around them (e.g., Puffin and Alcyon;
324 Fig. 9, 12d & 12e). But generally these local responses to diapiric rise were masked by

325 large changes in regional thickness controlled by crustal tectonics. As the source layer
326 depleted and the salt was partially welded, many salt diapirs stopped growing in the
327 mid-Cretaceous.

328

329 **Effect of basement structures on early salt tectonics**

330 North-dipping faults (Ibis and Landes faults) offsetting the basement with
331 throws of more than 3 km are recognizable in the southern boundary of the basin.
332 However, smaller faults are largely masked by the velocity effects of salt. Also,
333 Pyrenean inversion may have removed early extensional offset on smaller faults.
334 Despite poor imaging, the huge scale of faulting means that basement tilting and fault
335 offsets evidently controlled the initial thickness of salt and overburden and hence
336 affected the style of salt tectonics. Contrasting effects are shown by the Ibis Fault and
337 the Landes Fault.

338

339 *Ibis Fault*

340 The most important structure of the eastern Parentis Basin is the Ibis Fault, which is
341 overlain by the Eridan-Antares anticline. In the southern limb of the anticline the
342 Jurassic-Cretaceous transition is marked by the southwards thinning and the onlap of
343 Lower Cretaceous strata. These features suggest that the Ibis footwall was already
344 elevated and tilted northward at the start of the Cretaceous (Fig. 6 shows the present-day
345 subhorizontal attitude after Paleogene rotation of the basement during inversion).
346 Farther south near the edge of the basin, this thinning changes to a strongly erosive
347 regional unconformity. North of the Eridan-Antares anticline, thickening of the
348 Neocomian to lower Aptian sequences suggests that the Parentis Trough began its main
349 subsidence in Neocomian times.

350 Although the basement is poorly imaged, the Ibis Fault is interpreted as a half
351 graben because its overburden forms a monocline verging northward (Figs. 4A & 6). A
352 salt-cored anticline (Eridan-Antarés anticline) drapes over the northward-dipping master
353 fault of the half graben. Generic physical modeling (e.g. Withjack and Callaway, 2000;
354 Ferrer et al., 2008b) suggests that before Pyrenean shortening, this anticline was
355 probably a monoclinial extensional drape fold responding to slip on the underlying Ibis
356 Fault. The viscous salt layer partially decoupled the major sub-salt fault slip from the
357 draping cover. Physical modeling (Jackson et al., 1994; Vendeville et al., 1995;
358 Withjack and Callaway, 2000) suggests that in such systems, the displacement and
359 displacement rate of the sub-salt normal fault and the thickness and strength of the salt
360 layer and its overburden controlled the structural style of the cover sequence. Thrust
361 faults similar to those in the northern limb of the fold also form in physical models of
362 drape monoclines above a rapidly slipping normal fault in the basement (Withjack and
363 Callaway, 2000).

364 A massive upper Aptian-Albian depocentre on the north flank of the Eridan-
365 Antarés anticline onlaps markedly onto the Céphée-Aldebaran anticline to its north
366 (Figs. 4A, 6 & 12d). The main sedimentary load of the Parentis Trough was thus
367 confined between the two salt-cored anticlines. This differential load in the trough
368 would have expelled salt laterally to the north and south and possibly to the east, where
369 overburden was thinner. Salt expulsion would have allowed the depocenter to subside
370 and eventually weld the autochthonous salt beneath the base of the trough, as inferred in
371 Figures 4A and 6.

372

373 *Landes Fault*

374 The Landes Fault forms a half-graben at the southern edge of the Triassic salt basin and
375 its overburden 5000-8500 m thick. Basement dips southwards in the hanging wall and
376 farther north is near-horizontal or gently northward dipping (Fig. 4B). This change in
377 hanging-wall dip strongly influenced the location and evolution of the Txipiroi salt-
378 cored anticline (Ferrer *et al.*, 2008a) at the edge of the half-graben. Uppermost
379 Cretaceous-Cenozoic strata rest on an angular unconformity, especially above
380 extensional tilted blocks. Erosion truncated more than half the Lower Cretaceous
381 sediment thickness below the severest parts of the unconformity (Fig. 9). Fault
382 geometry suggests that the Txipiroi anticline grew from the migration and later
383 accumulation of Keuper salt (Ferrer *et al.*, 2008a & Ferrer *et al.*, 2008b).

384 As extension, basement tilting and sedimentation progressed during the Jurassic
385 and Early Cretaceous, increased loading of the Landes half-graben expelled salt into
386 early-formed diapirs such as Euskal Balea and Izurde and laterally to the north up the
387 tilted hanging wall of the Landes Fault (Fig. 9). Lateral salt migration produced salt-
388 cored anticlines where the dip of the basement becomes near-horizontal, forming the
389 Txipiroi and Izurde ridges (Ferrer *et al.*, 2008b). Salt migration ended when the source
390 layer welded. Examples of similar structural style have been described in the Jeanne
391 d'Arc basin (Withjack & Callaway, 2000 & Ferrer *et al.*, 2010).

392

393 **Pyrenean shortening of salt structures**

394 The Pyrenean orogeny began during the Late Cretaceous and continued to the
395 Eocene. As a result the central part of the Parentis Basin (Parentis Trough) was uplifted
396 and inverted (Fig. 12e). The top of Cretaceous was strongly eroded, and the Paleocene
397 unit is higher than south of the Ibis Fault (Figs. 6 & 12f). The Parentis Basin as a whole
398 was only mildly shortened by this orogeny compared with the Pyrenean hinterland

399 where the minimum total shortening is about 165 km (Beaumont *et al.*, 2000 & Muñoz,
400 2002).

401 The Landes High in the Parentis Basin appears to have provided a buttress against the
402 Pyrenean compression, which protected the Parentis Basin from major inversion even
403 though the underlying crust was severely thinned in the Mesozoic (Ferrer *et al.*, 2008a).
404 The lack of significant inversion structures in the Parentis Basin is the main indication
405 that the Landes High shielded the Parentis Basin from Pyrenean shortening from Late
406 Cretaceous to Early Miocene time. Shielding explains why basement-involved Pyrenean
407 shortening is only present south of the Landes High and concentrated along the northern
408 margin of the Basque-Cantabrian Basin (Fig. 1C). The Landes High acted as a buttress
409 probably because it had a stronger crust than in the adjoining Basque-Cantabrian and
410 Parentis basins. The two basins were strongly extended in the Early Cretaceous, so that
411 thin, warm crust was overlain by thick Mesozoic cover. By contrast in the Landes High,
412 where Mesozoic extension was much less, the crust was thicker and colder and overlain
413 by thin cover and thus significantly stronger and able to resist Pyrenean compression
414 along the Iberian-Eurasia collision boundary.

415 The Pyrenean inversion of the Parentis Basin drastically deformed salt structures
416 formed earlier by Triassic-Early Cretaceous extension and halokinesis. Most salt
417 structures responded readily to shortening by rising and narrowing because they were
418 weak and their ENE trend was favorably oriented to the north-directed Pyrenean
419 compression (Figs. 11 & 12f). Salt structures responded in the following ways. (1)
420 Previously buried and dormant salt walls near the southern boundary of the basin were
421 rejuvenated by squeezing as the salt within them was displaced upwards and arched
422 their previously flat-lying roofs (Figs. 8, 10, 11 & 12f). (2) Squeezed salt walls extruded
423 so much that salt advanced glacially, beginning in the lattermost Cretaceous and

424 accelerating during Eocene-early Miocene times (Figs. 7 & 11). (3) Large anticlines
425 rose above regional during shortening as the salt-cored Ibis and Eridan-Antarés ridges
426 above the Ibis Fault and the Txipiroi anticline near the Landes Fault (Figs. 4A & 4B).
427 (4) In the most extreme regional shortening, both extruding and buried salt walls could
428 have pinched off to form subvertical secondary salt welds (Figs. 10, 11, 12f & 12g). If
429 diapirs welded shut, any further shortening could have been by inversion of pre-existing
430 normal faults, by reverse fault welds or by short-cut thrusts that nucleated in the salt
431 pedestals during the last stages of the Pyrenean contraction (Fig. 8). No new diapirs
432 formed during the inversion because the source layer was largely depleted in salt. Salt
433 diapirism ended with the close of the Pyrenean orogeny in the middle Miocene (Figs. 9,
434 10, 11 & 12g).

435 Pinching off of some diapirs is conjectural but is suggested by these three lines
436 of evidence, each of which is disputable. (1) Pinch-off is mechanically likely as the
437 culmination of shortening in a wide array of geological settings (e.g., Vendeville &
438 Nilsen, 1995; Cramez & Jackson, 2000; Brun & Fort, 2004; Gottschalk *et al.*, 2004;
439 Rowan *et al.* 2004; Roca *et al.*, 2006; Rowan & Vendeville, 2006; Sherkati *et al.*, 2006;
440 Jackson *et al.*, 2008; Dooley *et al.*, 2009). However, shortening may not have been
441 sufficient for complete pinch off. (2) In the western Parentis Basin, where the quality of
442 seismic data is better, the strong reflector of the top of autochthonous salt curves up to a
443 cusped point below the crest of the salt wall. However, this geometry could be a
444 velocity pull-up. (3) The roof of the diapirs is arched above the regional in some places,
445 as for Puffin Diapir in Figure 6. Where one side of the diapir is uplifted higher than the
446 other side, this is compatible with a thrust-weld resulting from closure of an inclined
447 stem. Again, though the asymmetrical arching could reflect another cause: namely an
448 inclined stream rising up the inclined stem of a diapir.

449

450 **Conclusions**

451 The evolution of the Parentis Basin during extensional and subsequent
452 contractional crustal deformation was strongly influenced by salt tectonics. Two master
453 faults (Ibis and Landes faults) separated two structural domains having a wide array of
454 salt-related structures. These faults may form a large relay structure. Salt stocks and
455 walls grew near the south edge of the salt basin in the hanging wall of the Landes Fault
456 in the western domain and in the footwall of the Ibis Fault in the eastern. In the east,
457 gentle drape anticlines cored by salt formed in the edges of the basin (Eridan-Antares-
458 Ibis and Céphée-Castor ridges). In the west, larger salt-cored anticlines formed in the
459 crest of basement antiforms (e.g. Txipiroi salt-anticline) or above flat basement (e.g.
460 Marratxo and Izurde salt-anticlines).

461 Salt walls and diapirs rose from a Triassic source layer deposited during Pangea
462 rifting. These structures may have been initiated in extension as reactive diapirs during
463 early opening of the Bay of Biscay or by differential sedimentary loading as early as the
464 Upper Jurassic. The thick sedimentary fill deposited in the Parentis Trough since the
465 Barremian to Albian expelled Keuper evaporites towards the edges of the basin where
466 salt-cored anticlines formed. The Eridan-Antares-Ibis anticline grew as a drape fold
467 above the Ibis master fault in response to its slip. The Céphée-Castor salt-cored
468 anticline grew in the northern edge.

469 Salt diapirs evolved to a passive mode during Albian times. Many of these walls
470 stopped growing by the middle of the Late Cretaceous, but some continued to grow
471 passively until the Miocene.

472 As Iberia and Eurasia collided and drove the Pyrenean orogeny in the Late
473 Cretaceous, the Parentis Basin was mildly shortened. Pre-existing salt-cored anticlines
474 were amplified so that their crests were uplifted and eroded. Because of their weakness
475 and preferred orientation, most salt structures responded readily to compression and
476 absorbed most of the Pyrenean shortening. Diapirs, some of which were dormant and
477 buried, were rejuvenated by regional compression as their stems may have pinched off.
478 Upward expulsion of salt displaced from the squeezed walls arched up their sedimentary
479 roofs to form shallow anticlines. Locally the pre-shortening salt walls expelled salt
480 which advanced as glaciers over the sea floor for up to 20 km. This salt sheet stopped
481 advancing and was buried during the Oligocene. No new diapirs formed as the Parentis
482 Basin was inverted because the autochthonous source layer was largely depleted.

483

484 **Acknowledgements**

485

486 Our work was financially supported by the MARCONI (REN2001-1734-C03-
487 02/MAR), the GEOMOD 4D (CGL2007-66431-C02-02/BTE) and the INKISAL
488 (CGL2010-21968-C02-01) projects and the “Grup de Recerca de Geodinàmica i Anàlisi
489 de Conques” (2001SRG-000074). Research by O. Ferrer is funded by a predoctoral
490 grant from the Ministerio de Educación, Cultura y Deporte (AP2002-0988). The authors
491 thank *Hidrocarburos de Euskadi* for providing data and particularly to J. García and A.
492 Frankovic. Special thanks to M. R. Hudec and J. A. Cartwright for fruitful discussions
493 and help during the interpretation of the seismic data while O. Ferrer was a visiting
494 scientist at the Bureau of Economic Geology. The authors acknowledge support of this
495 research by Landmark Graphics Corporation via the Landmark University Grant
496 Program. The seismic interpretation also used Kingdom Suite software, which was

497 generously provided by Seismic Micro-Technology. Midland Valley provided 2DMove,
498 which was used for the cross-section restoration. MJ was supported by the Applied
499 Geodynamics Laboratory consortium. The paper is published by permission of the
500 Director, Bureau of Economic Geology. Finally we gratefully acknowledge Editor I.
501 Alsop and M. Rowan and M. Albertz, whose reviews significantly improved the
502 manuscript.

503

504 **References**

505

506 Álvarez-Marrón, J., Pérez-Estaún, A., Dañobeitia, J.J., Pulgar, J.A., Martínez Catalán, J.R., Marcos, A.,
507 Bastida, F., Ayarza Arribas, P., Aller, J., Gallart, A., Gonzalez-Lodeiro, F., Banda, E., Comas,
508 M.C. & Córdoba, D. 1996. Seismic structure of the northern continental margin of Spain from
509 ESCIN deep seismic profiles. *Tectonophysics*, **264**, 153-174.

510 Ayarza, P., Martínez-Catalán, J.R., Álvarez-Marrón, J., Zeyen, H. & Juhlin, C. 2004. Geophysical
511 constraints on the deep structure of a limited ocean-continent subduction zone at the North Iberian
512 Margin. *Tectonics* **23**, TC1010, doi:10.1029/2002TC001487

513 Beaumont, C., Muñoz, J. A., Hamilton, J. & Fullsack, P. 2000. Factors controlling the Alpine evolution of
514 the central Pyrenees inferred from a comparison of observations and geodynamical models.
515 *Journal of Geophysical Research*, **105**, 8121-8145.

516 Biteau, J.J., Le Marrec, A., Le Vot, M. & Massot, J.M. 2006. The Aquitaine Basin. *Petroleum Geoscience*
517 **12**, 247-273.

518 Boillot, G. 1986. Le Golfe de Gascogne et les Pyrénées, *In*: Boillot, G. (ed.), *Les marges continentales*
519 *actuelles et fossiles autour de la France*. Mason, Paris, 5-81.

520 Bois, C. & Gariel, O. 1994. Deep seismic investigation on the Parentis Basin (Southwestern France) *In*:
521 Mascle A. (ed.) *Hydrocarbon and petroleum geology of France*. European Association of
522 Petroleum Geologist, Special publication, **4**, 173-186.

523 Bois, C., Pinet, B. & Gariel, O. 1997. The sedimentary cover along the ECORS Bay of Biscay deep
524 seismic reflection profile. A comparison between the Parentis Basin and other European rifts and
525 basins. *Mémoires de la Société Géologique de France* **171**, 143-165.

- 526 Bois, C. & ECORS Scientific Party. 1990. Major geodynamic processes studied from the ECORS deep
527 seismic profiles in France and adjacent areas. *In: Leven, J.H. Finlayson, D.M. Wright, C. Dooley*
528 *J.C. & Kennet B.L.N. (eds) Seismic probing of continents and their margins. Tectonophysics, 173,*
529 *397-410.*
- 530 Bourrouilh, R., Richter, J.P. & Zolnai, G. 1995. The North Pyrenean Aquitaine Basin, France: Evolution
531 and Hydrocarbons. *American Association of Petroleum Geologist Bulletin* **79**, 831-853.
- 532 Brun, J.P. & Fort, X. 2004. Compressional salt tectonics (Angolan Margin). *Tectonophysics, 382,* 129-
533 150.
- 534 Brunet, M.F. 1991. Subsidence in the Parentis Basin (Aquitaine, France): implications of the thermal
535 evolution. *In: Mascle, A. (ed.) Hydrocarbon Exploration and Underground Gas Storage in*
536 *France. Springer Verlag. Paris, 4, 187-198.*
- 537 Callot, J. P., Jahani, S. & Letouzey, J. 2007. The role of pre-existing diapirs in fold and thrust belt
538 development. *In: Lacombe, O., Roure, F., Lavé, J. & Verges, J., (eds) Thrust belts and foreland*
539 *basins from fold kinematics to hydrocarbon systems: Frontiers in earth sciences. Springer, Berlin,*
540 *Heidelberg, p. 309–325.*
- 541 Choukroune, P. & ECORS Team. 1989. The ECORS Pyrenean deep seismic profile: Reflection data and
542 the overall structure of an orogenic belt. *Tectonics, 8 (1), 23-39.*
- 543 Cramez, C. & Jackson, M.P.A. 2000. Superposed deformation straddling the continental-oceanic
544 transition in deep-water Angola. *Marine and Petroleum Geology. 17,* 1095-1109.
- 545 Cumelle, R., Dubois, P. & Seguin, J.C. 1982. The Mesozoic-Tertiary evolution of the Aquitaine basin.
546 *Philosophical Transactions of the Royal Society of London, A305,* 63-84.
- 547 Cumelle, R., & Cabanis, B. 1989. Relations entre le magmatisme « triasique » et le volcanisme infra-
548 liasique des Pyrénées et de l'Aquitaine ; Apports de la géochimie des éléments en traces. *Bulletin*
549 *Centre de Recherches Exploration-Production Elf-Aquitaine, 13,* 347-375.
- 550 Cumelle, R. & Marco, R. 1983. Reflection profiles across the Aquitaine basin, *In: Bally, A.W. (ed.), A*
551 *Picture and work atlas. Seismic Expression of Structural Styles. American Association of*
552 *Petroleum Geologists. Studies in Geology, 2.3.2-11 – 2.3.2.-17.*
- 553 Dardel, R.A. & Rosset., R. 1971. Histoire géologique et structurale du bassin de Parentis et de son
554 prolongement en mer, *In: Debyser, J. Le Pichon, X. & Montadert, L. (eds) Histoire Structurale du*

- 555 *Golfe de Gascogne*. Publication de l'Institut Français du Pétrole. Technip. Paris, I, IV.2.1. -
556 IV.2.28.
- 557 Derégnaucourt, D. & Boillot, G. 1982. Structure géologique du golfe de Gascogne. *Bulletin du Bureau de*
558 *Recherches Géologiques et Minières de France* **1**, 149-178
- 559 Dooley, T. P., Jackson, M. P. A. & Hudec, M. R. 2009. Inflation and deflation of deeply buried salt
560 stocks during lateral shortening. *Journal of Structural Geology*, **31**, 582-600.
- 561 Ferrer, O., Roca, E., Benjumea, B., Muñoz, J.A., Ellouz, N. & MARCONI Team. 2008a. The deep
562 seismic reflection MARCONI-3 profile: Role of extensional Mesozoic structure during the
563 Pyrenean contractional deformation at the Eastern part of the Bay of Biscay. *Marine and*
564 *Petroleum Geology*, **25**, 714-730.
- 565 Ferrer, O., Vendeville, B.C. & Roca, E. 2008b. Influence of a syntectonic viscous layer on the structural
566 evolution of extensional kinked-fault systems. *Bolletino di Geofisica teorica ed applicata*, **49**, 371-
567 375.
- 568 Ferrer, O., Mencos, J., Roca, E. & Muñoz, J. A. 2010. Kinematics of inversion salt tectonics along the
569 Newfoundland – Bay of Biscay – Pyrenean Rift System: comparison between the preserved rift
570 segments and the inverted ones. *GSL-SEPM Conference – Salt Tectonics, Sedimentation, and*
571 *Prospectivity*, 68.
- 572 Fletcher, R.C., Hudec, M.R. & Watson, I. A. 1995. Salt glacier and composite sediment-salt glacier
573 models for the emplacement and early burial of allochthonous salt sheets. *In: Jackson, M.P.A.,*
574 *Roberts, D.G., Snelson, S. (eds) Salt Tectonics: A Global Perspective. American Association of*
575 *Petroleum Geologists Memoir* **65**, 77–108.
- 576 Gallart, J., Pulgar, J.A., Muñoz, J.A. & MARCONI Team. 2004. Integrated studies on the lithospheric
577 structure and Geodynamics of the North Iberian Continental Margin: The MARCONI Project.
578 *Geophysical Research Abstracts*, **6**, 04196, SRef-ID: 1607-7962/gra/EGU04-A04196. European
579 Geosciences Union.
- 580 Gallastegui, J., Pulgar, J.A. & Gallart, J. 2002. Initiation of an active margin at the North Iberian
581 continent-ocean transition. *Tectonics* **21** (4), 10.1029/2001TC901046.
- 582 García-Mondejar, J. 1996. Plate reconstruction of the Bay of Biscay. *Geology*. **24**(7), 635-638.
- 583 Gariel, O, Bois, C., Curnelle, R., Lefort, J.P. & Rolet, J. 1997. The ECORS Bay of Biscay deep seismic
584 survey. Geological framework and overall presentation of the work. *In: Mémoires de la Société*

585 Geologique de France (ed) *Deep seismic study of the Earth's crust. ECORS Bay of Biscay Survey.*
586 Paris, 7-19.

587 Giles, K.A. & Lawton, T.F. 2002. Halokinetic sequence stratigraphy adjacent to the El Papalote diapir,
588 northeastern Mexico. *AAPG Bulletin*, **86**, 823–840.

589 Gottschalk, R. R., Anderson, A. V., Walker, J. D. & Da Silva, J. C., 2004. Modes of contractional salt
590 tectonics in Angola Block 33, Lower Congo basin, West Africa. *In: Post, P. J., Olson, D. L., Lyons,*
591 *K. T., Palmes, S. L., Harrison, P. F. & Rosen, N. C. (eds) Salt-Sediment Interactions and*
592 *Hydrocarbon Prospectivity: Concepts, Applications, and Case Studies for the 21st century*, 24th
593 Annual Research Conference. SEPM Foundation, 705-734.

594 Hudec, M.R. & Jackson, M.P.A. 2006. Advance of allochthonous salt sheets in passive margins and
595 orogens. *AAPG Bulletin*, **90(10)**, 1535-1564.

596 Hudec, M.R. & Jackson, M.P.A. 2007. Terra infirma: Understanding salt tectonics. *Earth-Science*
597 *Reviews*, **82**, 1-28.

598 Jackson, M. P.A. 1995. Retrospective salt tectonics. *In: Jackson, M.P.A., Roberts, D.G. & Snelson, S.*
599 *(eds) Salt tectonics: a global perspective. American Association of Petroleum Geologist Memoir,*
600 **65**, 1-28.

601 Jackson M.P.A. & Cramez, C. 1989. Seismic recognition of salt welds in salt tectonics regimes.
602 *GCSSEPM Foundation Tenth Annual Research conference. Program and Abstracts*, 66- 71.

603 Jackson, M. P. A., Hudec, M.R., Jennette, D. C. & Kilby, R.E. 2008. Evolution of the Cretaceous Astrid
604 thrust belt in the ultradeep-water Lower Congo Basin, Gabon. *American Association of Petroleum*
605 *Geologists Bulletin*, **92**, 487–511.

606 Jackson, M.P.A, Vendeville, B.C. & Schultz-Ela, D.D. 1994. Structural dynamics of salt systems. *Annual*
607 *Review of Earth and Planetary Sciences*, **22**, 93–117.

608 Le Pichon, X. & Barbier, F. 1987. Passive margin formation by low-angle faulting within the upper crust:
609 the northern Bay of Biscay margin. *Tectonics*, **6**, 133-150.

610 Letouzey, J. & Sherkati, S. 2004. Salt movement, tectonic events, and structural style in the central
611 Zagros fold and thrust belt (Iran) : *24th Annual Research Conference SEPM Foundation*, 4444–
612 463.

- 613 Letouzey, J., Colletta, B., Vially, R. & Chermette, J. C. 1995. Evolution of salt-related structures in
614 compressional settings. *In: Jackson, M. P. A., Roberts, D. G. & Snelson, S. (eds) Salt tectonics – a*
615 *global perspective*. AAPG Memoir **65**, 41-60.
- 616 Le Vot, M., Biteau, J.J. & Masset, J.M. 1996. The Aquitaine Basin: Oil and gas production in the foreland
617 of the Pyrenean fold-and-thrust belt. New exploration perspectives. *In: Siegler, P.A. & Horyàth, F.*
618 *(eds) Pery-Tethys Memoir 2: Structure and Prospects of Alpine Basins and Forelands. Mémoires*
619 *du Musée Nationale Histoire Naturele*, **170**, 159-171.
- 620 Mascle, A., Bertrand, G. & Lamiroux, Ch. 1994. Exploration for and production of oil and gas in France:
621 a review of the habitat, present activity and expected developments. *In: Mascle, A. (ed)*
622 *Hydrocarbon and Petroleum Geology of France*. Special Publications EAPG. 4, 3-28.
- 623 Masse, P. 1997. The early Cretaceous Parentis Basin (France). A basin associated with a wrench fault.
624 *Memoires de la Societé géologique de France*, **171**, 177-185.
- 625 Mathieu, C. 1986. Histoire géologique du sous-bassin de Parentis. *Bulletin des Centres Recherche*
626 *Exploration-Production Elf-Aquitaine*, **10(1)**, 22-47.
- 627 Mauriaud, P. 1987. Le Bassin d'Aquitaine. *Pétrole et Techniques*, **335**, 38-41.
- 628 Mediavilla, F. 1987. La tectonique salifère d'Aquitaine. Le Bassin de Parentis. *Pétrole et Techniques*,
629 **335**, 35-37.
- 630 Montadert, L., De Charpal, O., Roberts, D.G., Guennoc, P. & Sibuet, J.C. 1979. Northeast Atlantic
631 passive margins: rifting and subsidence processes. *In: Talwani, M., Hay, W. & Ryan, W.B.H.*
632 *(eds) Deep drilling results in the Atlantic Ocean Continental margin and paleoenvironment*,
633 American Geophysical Union, Wasington, 154-186.
- 634 Muñoz, J. A. 1992. Evolution of a continental collision belt: ECORS-Pyrenees crustal balanced section,
635 *In: McClay, K. R. (ed) Thrust Tectonics*, Chapman and Hall, London, 235-246.
- 636 Muñoz, J.A. 2002. The Pyrenees. *In: Gibbons, W. & Moreno, T. (eds) The Geology of Spain*. Geological
637 Society, London, 370-385.
- 638 Pedreira, D. 2004. *Estructura cortical de la zona de transición entre los Pirineos y la Cordillera*
639 *Cantábrica*. PhD thesis, Universidad de Oviedo.
- 640 Pinet, B., Montadert, L. & the ECORS Scientific Party. 1987. Deep seismic reflection and refraction
641 profiling along the Aquitaine shelf (Bay of Biscay). *Geophysical Journal Royal Astronomical*
642 *Society*, **89**, 305-312.

- 643 Purser, B. H. 1973. Sedimentation around bathymetric highs in the southern Persian Gulf, *In*: Purser, B.
644 H. (ed) *The Persian Gulf: Holocene carbonate sedimentation and diagenesis in a shallow*
645 *epicontinental sea*. New York, Springer-Verlag, 157–177.
- 646 Roberts, D.G. & Montadert, L. 1980. Contrast in the structure passive margin of the Bay of Biscay and
647 Rockall Plateau. *Philisophical Translations of the Royal Astronomy Society of London*, **294**, 97-
648 103.
- 649 Rosenbaum, G., Lister, G.S. & Duboz, C. 2002. Relative motions of Africa, Iberia and Europe during
650 Alpine orogeny. *Tectonophysics*, **359**, 117-129.
- 651 Roure, F., Choukroune, P., Berastegui, J.A., Muñoz, J.A., Villien, A., Matheron, P. Bareyt, M., Seguret,
652 M., Cámara, P. & Deramond, J. 1989. ECORS deep seismic data and balanced cross sections,
653 geometric constraints on the evolution of the Pyrenees. *Tectonics*, **8** (1), 41-50.
- 654 Rowan, M.G. & Vendeville, B.C. 2006. Foldbelts with early salt withdrawal and diapirism : Physical
655 model and examples from the northern Gulf of Mexico and the Flinders Ranges, Australia. *Marine*
656 *and Petroleum Geology*, **23**, 871-891
- 657 Rowan, M.G., Peel, F.J. & Vendeville, B.C. 2004. Gravity-driven foldbelts on passive margins. *In*:
658 McClay, K.R. (ed) *Thrust Tectonics and Hydrocarbon Systems. AAPG Memoir* **82**, 157-182.
- 659 Ruiz, M. 2007. *Caracterització estructural i sismotectònica de la litosfera en el Domini Pirenaico-*
660 *Cantàbric a partir de mètodes de sísmica activa i passiva*. PhD thesis, Universitat de Barcelona.
- 661 Sherkati, S., Letouzey, J. & Frizon de Lamotte, D. 2006. Central Zagros fold-thrust belt (Iran): New
662 insights from seismic data, field observations and sandbox modeling. *Tectonics*, **25**, TC4007,
663 doi:10.1029/2004TC001766.
- 664 Sibuet, J.C., Pautot, G. & Le Pichon, X. 1971. Interpretation structurale du golfe de Gascogne à partir des
665 profiles de sismique. *In*: Debyser, J., Le Pichon, X. & Montadert, L. (eds) *Histoire Structurale du*
666 *Golfe de Gascogne*. Publication de l'Institute Français du Pétrole, Technip. Paris. II, VI.10.1-
667 VI.10.1-VI.10.31.
- 668 Sibuet, J.C., Monti, S., Loubrieu, B., Mazé, J.P. & Srivastava, S. 2004a. Carte bathymétrique de
669 l'Atlantique nord-est et du Golfe de Gascogne. *Bulletin de la Société Géologique de France*.
670 **175**(5), 429-442.

- 671 Sibuet, J.C., Srivastava, S. & Spakman, W. 2004b. Pyrenean orogeny and plate kinematics. *Journal of*
672 *Geophysical Research*, **109** B08104, doi: 10.1029/2003JB002514.
- 673 Stefanescu, M., Dicea, O. & Tari, G. 2000. Influence of extension and compression on salt diapirism in its
674 type area, East Carpathians Bend area, Romania. *In: Vendeville, B., Mart, Y. & Vigneresse, J.L.*
675 *(eds) Salt, Shale and Igneous Diapirs in and around Europe*. Geological Society, London, Special
676 Publications, **174**, 131-147.
- 677 Stewart, S.A. 2007. Salt tectonics in the North Sea Basin: a structural style template for seismic
678 interpreters. *In: Ries, A. C., Butler, R. W. H. & Graham, R. H. (eds). Deformation of the*
679 *Continental Crust: The Legacy of Mike Coward*. Geological Society of London, Special Publications,
680 **272**, 361-396.
- 681 Srivastava S.P., Roest W.R., Kovacs L.C., Oakey G., Lévesque S., Verhoef J. & Macnab R. 1990. Motion
682 of Iberia since the Late Jurassic: Results from detailed aeromagnetic measurements in the
683 Newfoundland Basin. *Tectonophysics*, **184**, 229-260.
- 684 Thinon, I., Mathias, L., Réhault, J.P., Hirn, A., Fidalgo-González, L. & Avedik, F. 2003. Deep structure
685 of the Armorican Basin (Bay of Biscay): a review of Norgasis seismic reflection and refraction
686 data. *Journal of the Geological Society of London*, **160**, 99-116.
- 687 Tomassino, A. & Marillier, F. 1997. Processing and interpretation in the tau-p domain of the ECORS Bay
688 of Biscay expanding spread profiles. *Mémoires de la Société Géologique de France*, **171**, 31-43.
- 689 Vendeville, B.C., Ge, H. & Jackson, M.P.A. 1995. Scale models of salt tectonics during basement-
690 involved extension. *Petroleum Geoscience*, **1**, 179-183.
- 691 Vendeville, B.C. & Nilsen, K.T. 1995. Episodic growth of salt diapirs driven by horizontal shortening. *In:*
692 *Travis, C.J., Harrison, H., Hudec, M.R., Vendeville, B.C., Peel, F.J. & Perkins, B.F. (eds) Salt,*
693 *Sediment, and Hydrocarbons*. SEPM Gulf Coast Section 16th Annual Research Foundation
694 Conference, 285-295.
- 695 Vergés, J. & García-Senz, J. 2001. Mesozoic evolution and Cainozoic inversion of the Pyrenean Rift. *In:*
696 *Ziegler, P.A., Cavazza, W., Robertson, A.H.F. & Crasquin-Soleau, S. (eds) Peri-Tethys Memoir 6:*
697 *Peri-Tethyan Rift/Wrench Basins and Passive Margins*. Mémoires Museum National Histoire
698 Naturelle, **186**, 187-212.

- 699 Withjack, M. O. & Callaway, S. 2000. Active normal faulting beneath a salt layer: An experimental study
700 of deformation patterns in the cover sequence. *AAPG Bulletin*, **84(5)**, 627-651.
- 701 Ziegler, P.A. 1988. Evolution of the Arctic-North Atlantic and the Western Tethys. *AAPG Memoirs*, **43**,
702 p. 198.
- 703

704 **FIGURE CAPTIONS**

705 **Fig. 1.** (A) Location map of the Pyrenees and the Bay of Biscay (modified from [Muñoz,](#)
706 [2002](#)). (B) Simplified tectonic map of the Pyrenees and adjoining basins (modified from
707 [Ferrer et al., 2008a](#)). Location of Figure 3 is shown by the dashed rectangle. (C) Upper-
708 crustal transect through the eastern Bay of Biscay and adjoining northern part of the
709 Basque Pyrenees (modified from [Ferrer et al., 2008a](#)). Location is shown in (B).

710

711 **Fig 2.** Bathymetric map of the eastern Bay of Biscay (modified from [Sibuet et al.,](#)
712 [2004a](#)) showing the seismic and well data used in this work. For clarity there are only
713 included the names of the wells referenced in the manuscript: 1) Aldebaran, 2) Eridan,
714 3) Pingouin, 4) Ibis-2b and 5) Pelican.

715

716 **Fig. 3.** Simplified Cenozoic subcrop map of the offshore Parentis Basin showing the
717 main salt structures and faults. Thick black lines and numbers show location of seismic
718 profiles and line drawings in [Figs. 4A, 4B, 6, 7, 8, 9 and 10](#).

719

720 **Fig. 4.** Line drawings of interpreted deep seismic lines through the Parentis Basin. (A)
721 ECORS-Bay of Biscay seismic profile (modified from [Pinet et al., 1987](#)) and (B)
722 MARCONI-3 seismic profile (modified from [Ferrer et al. 2008a](#)). Deep crustal structure
723 is not to scale. See [Fig. 2](#) for location.

724

725 **Fig. 5.** Tectonostratigraphic chart of the Parentis Basin showing ages, lithologies,
726 tectonic events, and horizons interpreted in seismic lines (partially compiled from
727 [Mathieu, 1986; Mediavilla, 1987; Bourrouilh et al., 1995; Le Vot et al., 1996 and Biteau](#)
728 [et al. 2006](#)).

729

730 **Fig. 6.** (A) Seismic section and (B) and interpreted line drawing of a composite 2D
731 seismic profile in the eastern Parentis Basin showing four salt structures (Puffin and
732 Alcyon diapirs and Eridan-Antares and Céphée-Aldebaran ridges). Note the strong
733 erosional unconformity in the top of Cretaceous in the Eridan-Antares Ridge and the
734 lensoid Lower Cretaceous units. Welded feeders are conjectural. See Fig. 3 for location.

735

736 **Fig. 7.** (A) Seismic section and (B) and interpreted line drawing of a 2D seismic profile
737 of the eastern Parentis Basin showing the Pelican Salt Sheet. Welded feeders are
738 conjectural. See Fig. 3 for location.

739

740 **Fig. 8.** (A) Seismic section and (B) and interpreted line drawing of a seismic line in the
741 eastern Parentis Basin showing two diapirs with different growth histories. Both diapirs
742 grew passively during the Jurassic and Early Cretaceous. Puffin Ridge then stopped
743 growing and was buried beneath a wedge of Upper Cretaceous-Eocene sediments
744 probably because of thinner original salt closer to the margin of the salt basin. Later
745 Puffin Ridge was rejuvenated by inversion in the early Oligocene. Alcyon Diapir
746 continued to grow passively until the middle Miocene and must have also been
747 squeezed during the Oligo-Miocene inversion. The differential rotation values within
748 synkinematic strata are only for qualitative comparisons because the profile has not
749 been depth converted. See Fig. 3 for location.

750

751 **Fig. 9.** (A) Seismic section and (B) and interpreted line drawing of a seismic line across
752 the western Parentis Basin (deep offshore) showing two salt-cored anticlines and two
753 possibly welded diapirs. See Fig. 3 for location.

754

755 **Fig. 10.** Geometry of Cretaceous and Cenozoic sedimentary units in two anticlines
756 cored by squeezed diapirs in the hanging wall of the Landes Fault in the southern
757 Parentis Basin. Both diapirs grew as passive diapirs during the Jurassic and Early
758 Cretaceous. The diapirs then stopped growing and were buried beneath an Upper
759 Cretaceous roof. They were rejuvenated by inversion in the early Oligocene and again
760 uplifted during the Middle Miocene by contractional reactivation of the faults that
761 controlled early growth of the diapirs. The differential rotation values within
762 synkinematic strata are only for qualitative comparisons because the profile has not
763 been depth converted. See [Fig. 3](#) for location.

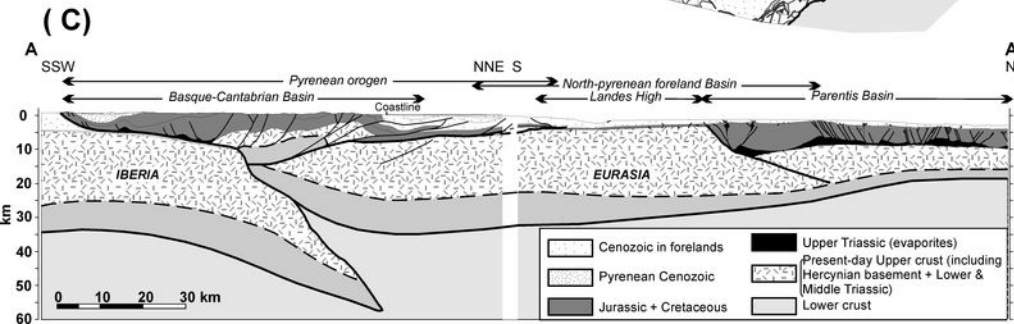
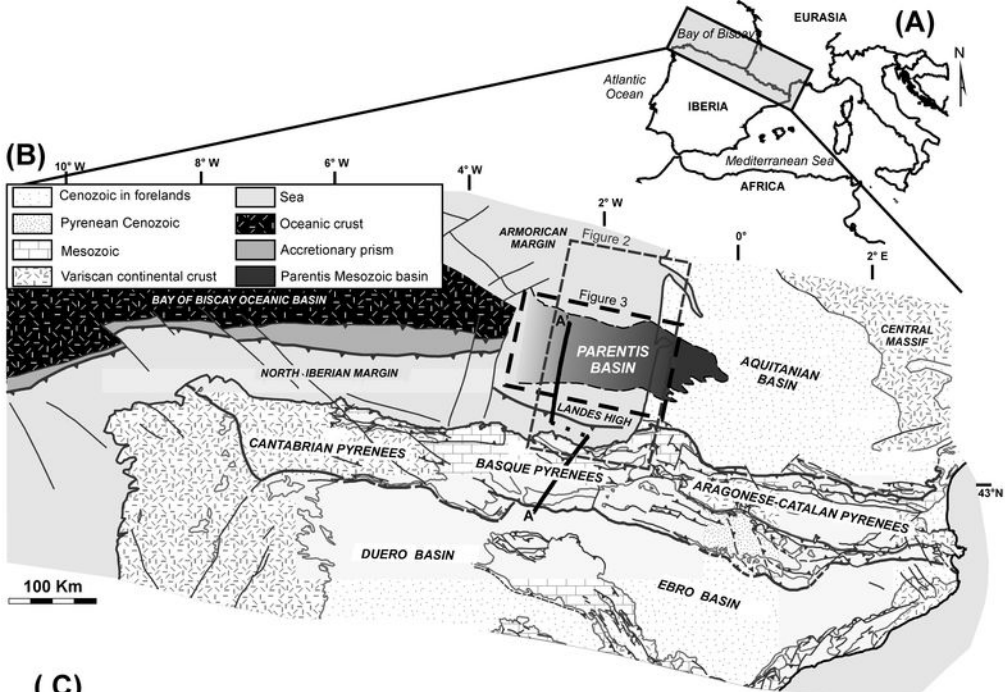
764

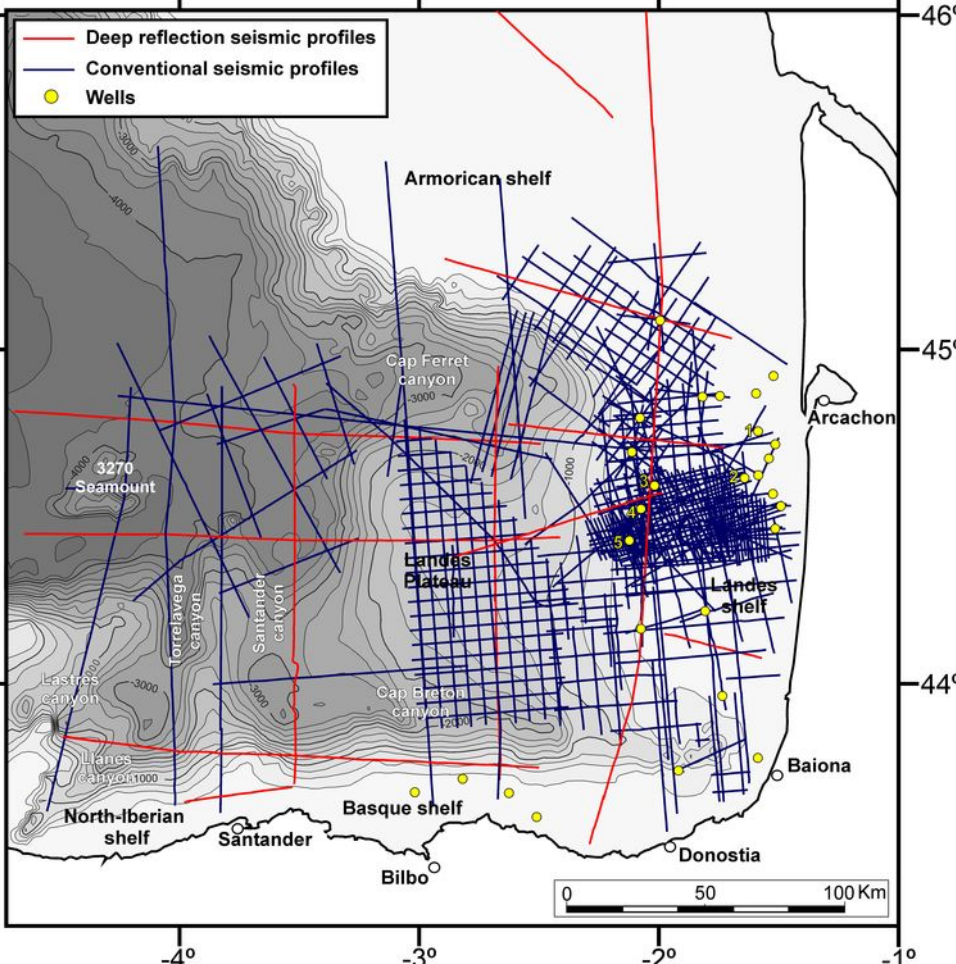
765 **Fig. 11.** Summary of the history of salt tectonics and regional tectonics in the offshore
766 Parentis Basin.

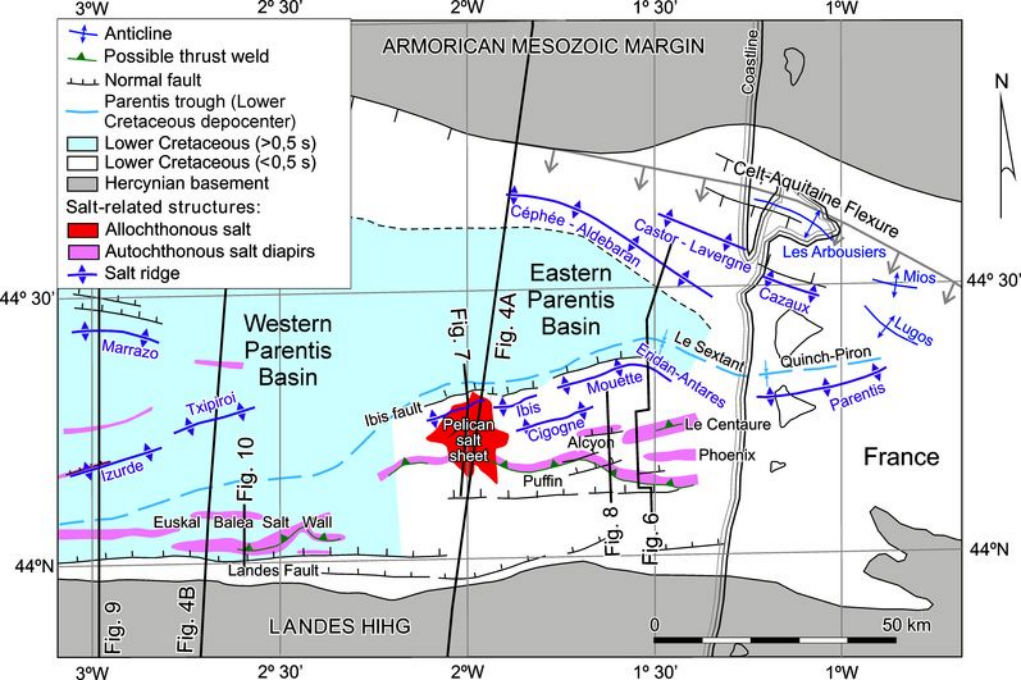
767

768 **Fig. 12.** Qualitative restoration of the eastern Parentis Basin regional profile showed in
769 [Fig. 6](#) using 2DMove software (see [Fig. 3](#) for location). (a) Evaporite deposition in the
770 Parentis Basin was bounded in the south by a basement high (Landes High) which also
771 controlled the thinning of the Jurassic package. (b-c) Extension produced a major
772 Barremian-Albian depocenter in the Parentis Trough which expelled Keuper evaporites
773 towards the north edge of the basin. A salt-cored anticline formed as a drape fold over
774 the Ibis Fault. (d-f) During the Pyrenean compression the drape fold above the Ibis Fault
775 was uplifted and its crest was eroded. In the south, previously buried, dormant salt walls
776 were rejuvenated by squeezing and arched their previously flat-lying roof (e.g. Puffin
777 Diapir). Later, buried salt walls may have pinched off by regional compression to form

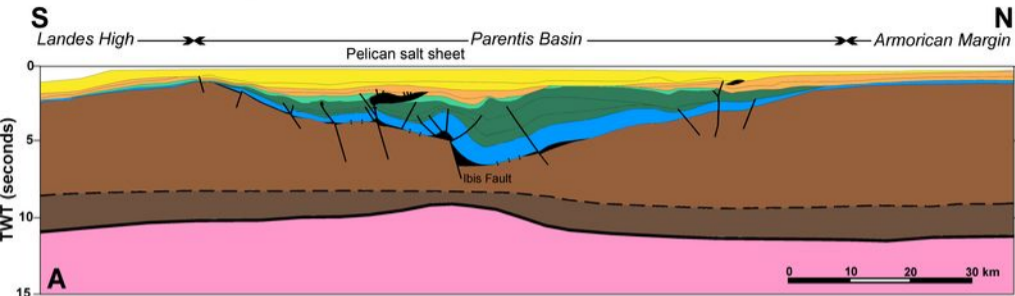
778 subvertical secondary salt welds (e.g. Alcyon Diapir). Salt tectonics ended during the
779 Miocene.



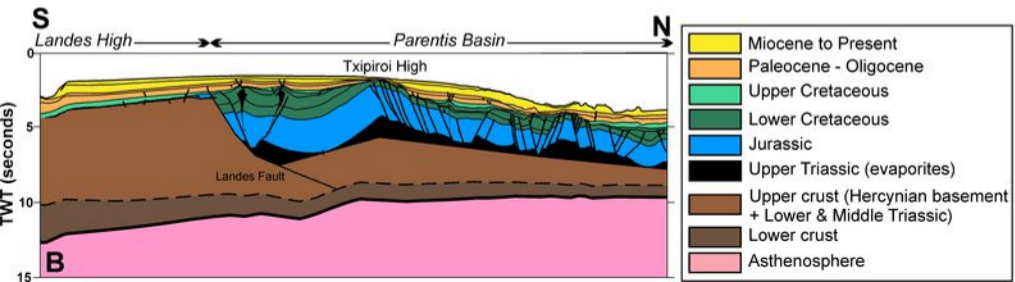


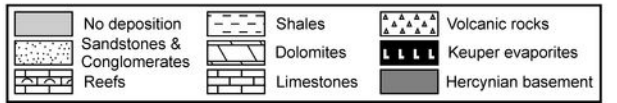
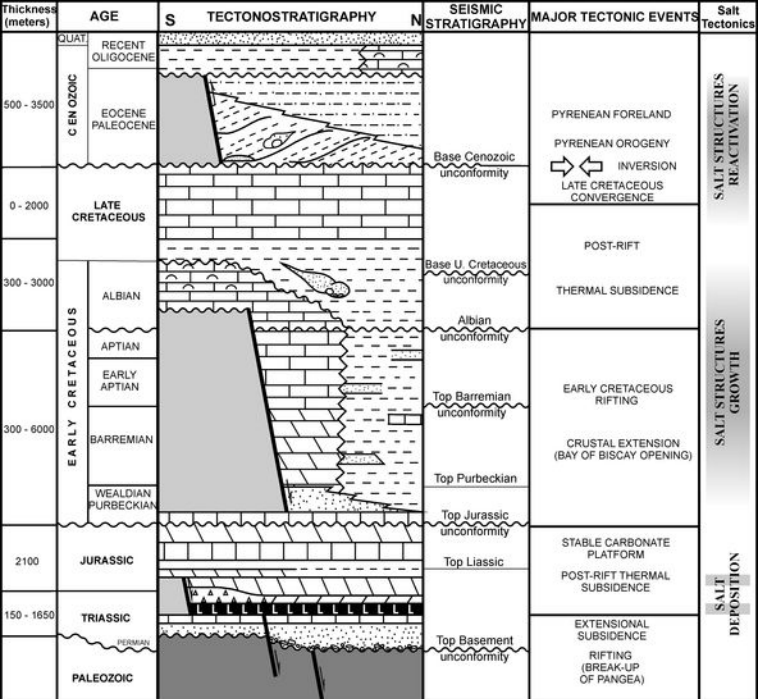


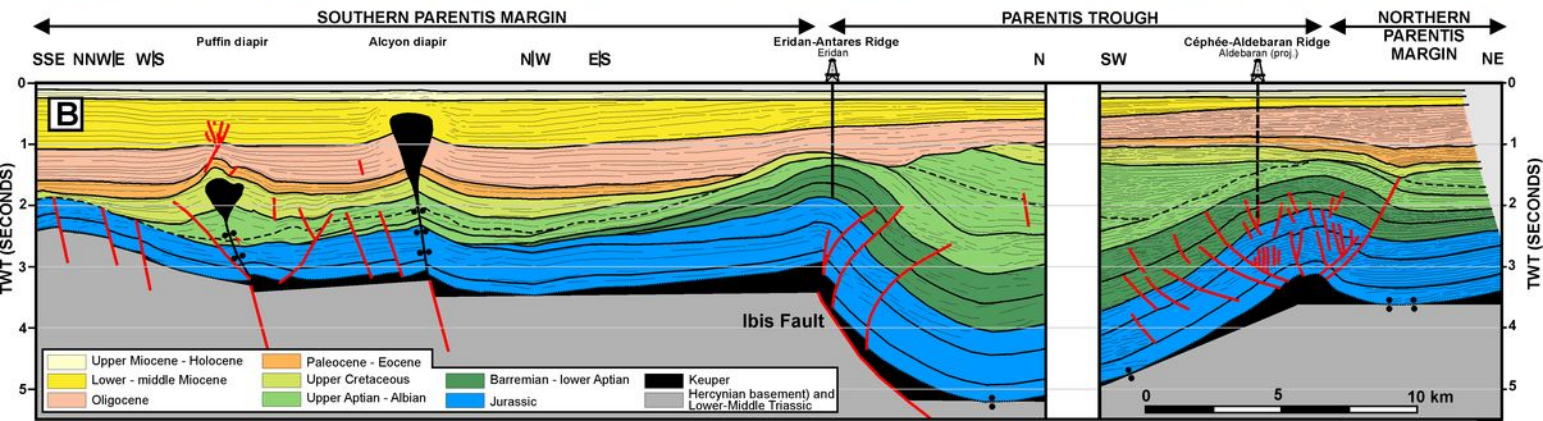
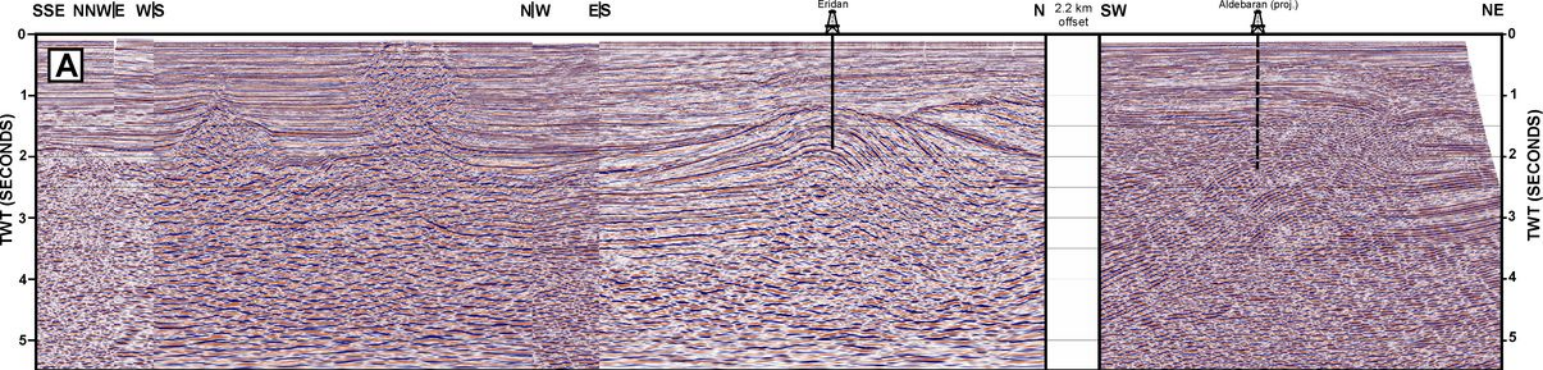
Cross section through Eastern Parentis Basin

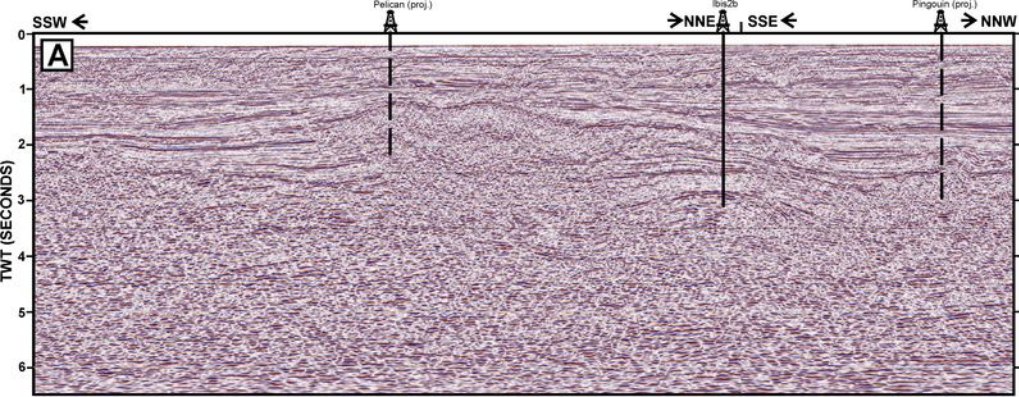


Cross section through Western Parentis Basin



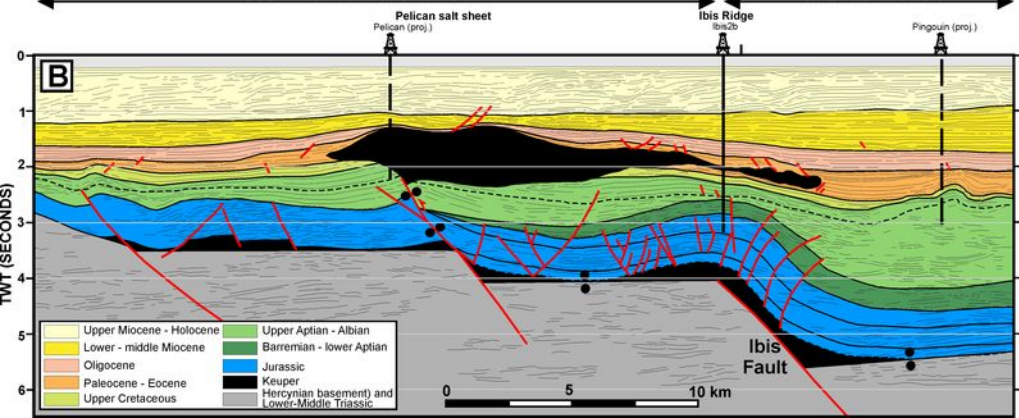


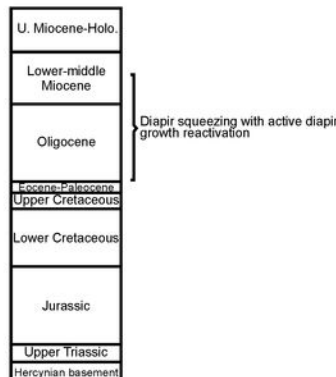
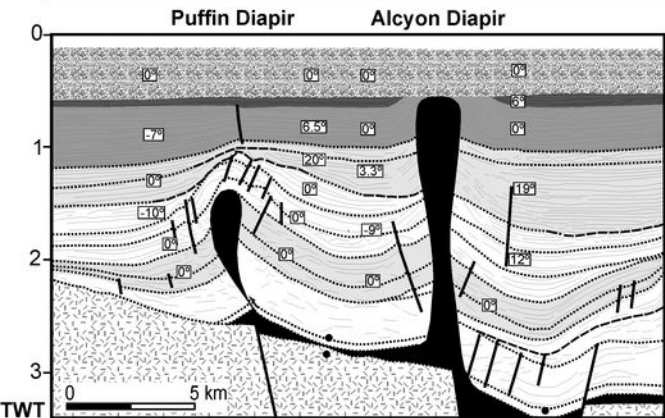
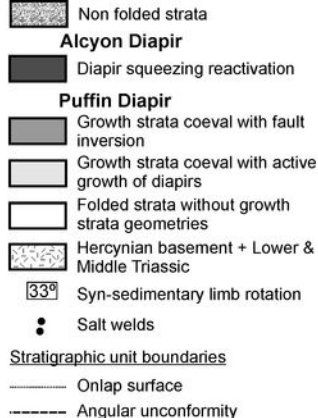
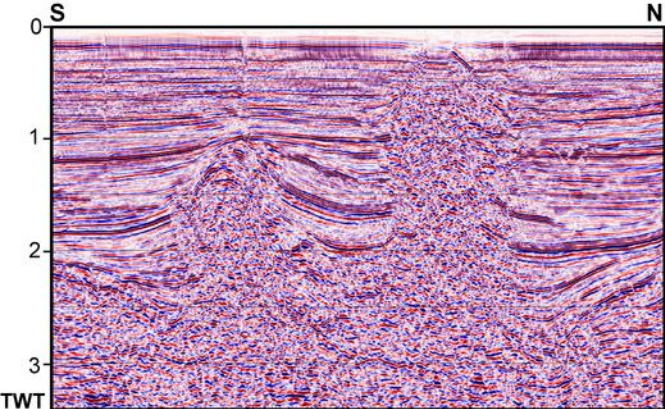


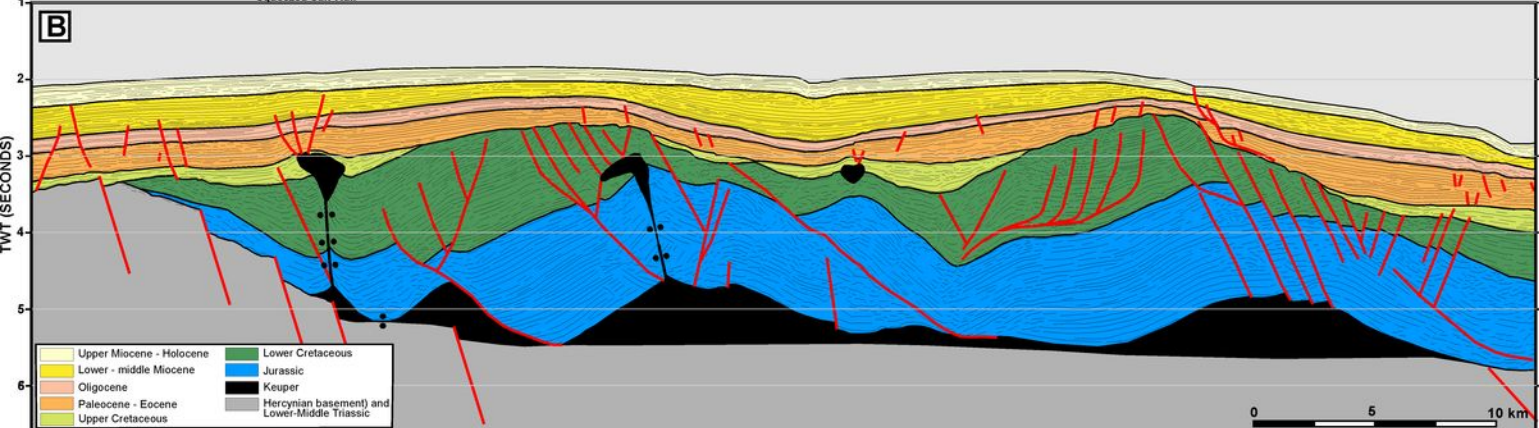
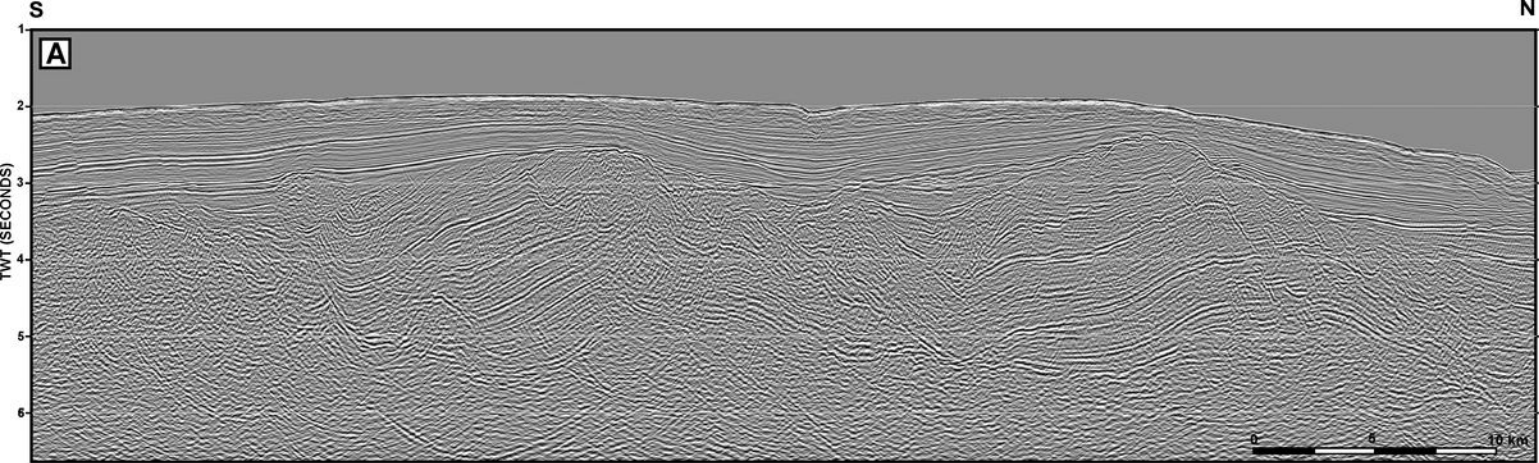


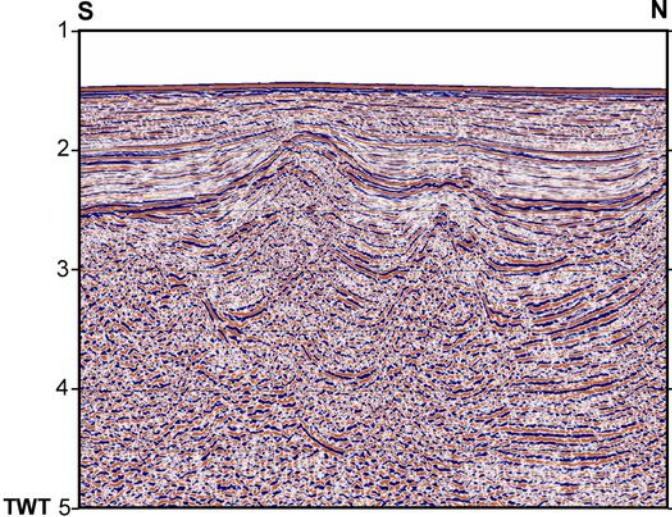
SOUTHERN PARENTIS MARGIN

PARENTIS TROUGH

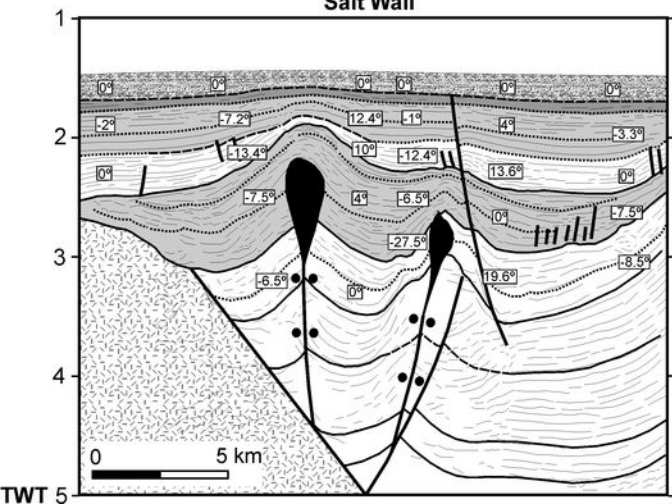








Euskal Balea Squeezed Salt Wall



U. Miocene-Holocene	} Fault inversion (uplift of the area between both diapirs) Diapir squeezing with active diapir growth reactivation
Middle Miocene	
L. Miocene-Oligocene	
Eocene-Paleocene	
Upper Cretaceous	} Diapir squeezing with active diapir growth reactivation
Albanian	
Barremian-Aptian	
Jurassic	
Upper Triassic	

